HYDROLOGICAL PROCESSES
Hydrol. Process. (2016)
Published online in Wiley Online Library
(wileyonlinelibrary.com) DOI: 10.1002/hyp.10792

Watershed structural influences on the distributions of stream network water and solute travel times under baseflow conditions

Anna Bergstrom,[1,2]* Brian McGlynn,[1] John Mallard[1] and Tim Covino[3]

[1] *Duke University, Division of Earth and Ocean Sciences, Nicholas School of the Environment, Durham, NC, USA*
[2] *University of Colorado-Boulder, Department of Civil Environmental and Architectural Engineering, Boulder, CO, USA*
[3] *Colorado State University, Ecosystem Science and Sustainability, Natural Resource Ecology Lab, Fort Collins, CO, USA*

Abstract:

Watershed structure influences the timing, magnitude, and spatial location of water and solute entry to stream networks. In turn, stream reach transport velocities and stream network geometry (travel distances) further influence the timing of export from watersheds. Here, we examine how watershed and stream network organization can affect travel times of water from delivery to the stream network to arrival at the watershed outlet. We analysed watershed structure and network geometry and quantified the relationship between stream discharge and solute velocity across six study watersheds (11.4 to 62.8 km^2) located in the Sawtooth Mountains of central Idaho, USA. Based on these analyses, we developed stream network travel time functions for each watershed. We found that watershed structure, stream network geometry, and the variable magnitude of inputs across the network can have a pronounced affect on water travel distances and velocities within a stream network. Accordingly, a sample taken at the watershed outlet is composed of water and solutes sourced from across the watershed that experienced a range of travel times in the stream network. We suggest that understanding and quantifying stream network travel time distributions are valuable for deconvolving signals observed at watershed outlets into their spatial and temporal sources, and separating terrestrial and in-channel hydrological, biogeochemical, and ecological influences on in-stream observations. Copyright © 2016 John Wiley & Sons, Ltd.

KEY WORDS stream network; solute transport; travel time

Received 18 September 2015; Accepted 15 January 2016

INTRODUCTION

Stream water characteristics observed at watershed outlets are the result of spatially distributed inflows to the stream network, in-channel processes, and channel network routing. Despite this, the roles of spatially variable inflows to the stream and network transport are seldom jointly considered in the interpretation of biogeochemical and hydrological parameters observed downstream. Interpretations of biogeochemical signals are particularly sensitive to solute transport pathways and travel times through the stream network that are not well represented by more commonly used kinematic velocities. We suggest that quantifying the distribution of stream network travel times as it is affected by variable inflows, in-channel routing, and solute transport velocities is critical to inferring and separating watershed and stream network processes.

Fundamental watershed characteristics can exert strong influences over the frequency distribution of travel times through stream networks. A stream network travel time distribution can be influenced by at least three main component processes: the spatial distribution of loading to the network (e.g. water, solutes, and particles) driven by upland watershed processes and structure, stream network travel distances from source areas to the watershed outlet (the stream network configuration), and the topology of stream network velocities. These components have been widely considered in the context of rainfall–runoff hydrologic response and flood wave modelling (e.g. Beven *et al.*, 1988; Gupta *et al.*, 1980; Moussa, 2008; Robinson *et al.*, 1995; Rodriguez-Iturbe and Valdes, 1979; Saco and Kumar, 2002a, b). These previous studies have made significant contributions to our understanding of how stream network geometry and watershed scaling properties can affect flood hydrographs. However, less progress has been made with regards to water molecule or solute travel times through stream networks.

Delivery of water to the stream network can be organized by watershed structure (the spatial arrangement

*Correspondence to: Anna Bergstrom, University of Colorado-Boulder, Department of Civil Environmental and Architectural Engineering, Boulder, CO, USA.
E-mail: abergst@gmail.com

of convergent and divergent hillslopes), in shallow soil systems with significant relief. For example, strongly convergent hillslopes with large upslope contributing or accumulated area typically deliver more water to the stream network than planar or divergent hillslopes with low upslope accumulated area under both baseflow and stormflow conditions (Anderson and Burt, 1978; Beven, 1978; Jencso *et al.*, 2009; Kirkby and Chorley, 1967; O'Loughlin, 1981; Speight, 1980). Locations in a watershed delivering more water to the stream network (larger lateral inflows (LIs)) can have a strong influence on streamwater composition observed at the watershed outlet because they have greater proportional contribution to discharge. To address this, some studies have used a 'normalized area function' to effectively incorporate the watershed area contributing water along the stream network (Robinson *et al.*, 1995; Snell and Sivapalan, 1994; Troutman and Karlinger, 1985). Accordingly, upland watershed structure can often be used to infer proportional contributions of water and solute signatures downstream.

The frequency distribution of stream network flowpath lengths to the watershed outlet, the width function, by itself is a useful watershed metric (Kirkby, 1976; Rinaldo *et al.*, 1995; Moussa, 2008; Lashermes and Foufoula-Georgiou, 2007) and a valuable tool for watershed classification and comparison (Moussa, 2008; Rinaldo *et al.*, 1995). It is frequently a core component of geomorphic instantaneous unit hydrograph type approaches to storm runoff hydrology (e.g. Gupta and Waymire, 1983; Rinaldo *et al.*, 1995; Snell and Sivapalan, 1994; Troutman and Karlinger, 1984). The width function can also represent stream travel distances that solutes take to the watershed outlet. Variable stream network path lengths to the watershed outlet lead to variations in stream network travel times and thereby geomorphic dispersion (Rinaldo *et al.*, 1991), even when velocity is assumed constant across the stream network. However, velocity is not uniform across stream networks, often because of differences in fluvial geometry and changes in stream discharge (Leopold and Maddock, 1953; Leopold, 1953; Leopold *et al.*, 1964; Pilgrim, 1976).

Streamflow velocities are often estimated with kinematic wave approximations of the Saint-Venant equations to describe the kinematic wave velocity (Lightbill and Whitham, 1955; McDonnell and Beven, 2014) as in many geomorphic instantaneous unit hydrograph type approaches. Studies have shown that spatially and temporally variable velocity (VV) can be useful for hydrologic response modelling (e.g. Agnese *et al.*, 1988; Lee and Yen, 1997; Saco and Kumar, 2002a, b; Snell *et al.*, 2004; Robinson *et al.*, 1995). These variable velocities contribute to spread in water arrival times, a process termed kinematic dispersion (Saco and Kumar, 2002a). Saco and Kumar (2002a) found that kinematic and geomorphic contributions to the dispersion of a kinematic wave were comparable, and both were significantly larger than influences from hydrodynamic dispersion. Kinematic velocity or celerity is distinct from solute transport velocity or tracer based velocity estimates that represent the downstream transport of water molecules and associated solutes rather than energy propagation (McDonnell and Beven, 2014). Specifically, kinematic velocity through a stream network is typically much faster than a solute or water molecule transport velocity (Graf, 1995; Luhmann *et al.*, 2012).

Solute transport velocities have been shown to increase with stream discharge (Calkins and Dunne, 1970; Covino *et al.*, 2011; Jobson, 1996; Pilgrim, 1976; Wondzell *et al.*, 2007). There are often positive relationships between stream discharge and conservative solute transport velocity across stream networks. This is exemplified by the compilation of studies presented in Wondzell *et al.* (2007) as well as in site-specific studies such as Calkins and Dunne (1970), Covino *et al.* (2011), and Funkhouser and Barks (2004). Despite this, most stream network scale studies concerned with solute transport often employ a constant velocity (CV) estimate, faster than a solute transport velocity, such as one derived from Manning's equation (e.g. Worrall *et al.*, 2013; Worrall *et al.*, 2014) or conversely use tracer (solute) velocity in place of kinematic velocity for stream discharge variations (e.g. Wondzell *et al.*, 2010). The choice of velocity approximation becomes an increasingly important distinction with longer distances and associated travel time scales (Graf, 1995).

In this study, we developed stream network travel time functions that consider spatially variable LIs of water and solutes to streams, variable stream network travel distances to the watershed outlet, and variable solute velocities across the stream network. We call these stream network travel time distributions Inflow Weighted, Variable Velocity, Travel Time Functions (IW-VV-TTFs). They describe the probability density function of stream network travel times for water molecules and conservative solutes after they have entered the stream network. We propose that these functions can inform interpretation of conservative solute observations and help interpret non-conservative biogeochemical and ecological parameters sensitive to in-channel processes, travel distances, and travel time in the fluvial network under non-stormflow conditions. We analysed six watersheds to investigate how (1) spatially variable network inflows, (2) network geometry, and (3) variable solute transport velocity individually and collectively can influence the distribution of stream network travel times.

METHODS

Study sites

We examined six watersheds located in the Sawtooth Mountains, central Idaho. These subalpine to alpine watersheds are all located within 70 km of each other, vary in size from 11.4 to 62.8 km^2, and range in elevation from 1988 to 3256 m (Table I). Terminal moraine lakes are present at study watershed outlets because of regional glaciation. Valley bottom fill is primarily composed of mixed Pleistocene till and Holocene colluvium and alluvium. Upland lithology is primarily granite and biotite granodiorite of the Idaho Batholith (Kiilsgaard *et al.*, 2003). Thirty-year average annual precipitation in the region is 108 cm, with 64% accumulating as snowfall (Banner Summit NRCS SNOTEL #312, 2140 m elevation located <2 km from Bull Trout and <50 km from other watersheds).

Field data collection and empirical relationship development

We conducted field experiments May–September in 2006 and 2007. Global positioning system surveys of stream networks were collected using a Trimble GeoXT global positioning system and differentially corrected using the Payette National Forest base station in McCall, ID (~120 km away). We used a combination of dilution gauging (e.g. Day, 1976) and velocity–area (e.g. Dingman, 2002) approaches to measure discharge (Q) within and across watersheds. The dilution gauging method is particularly effective in small streams with irregular channel cross-sections, while velocity-area gauging can be more accurate in larger streams with a more uniform cross section. Our discharge measurements consisted of instantaneous injections of sodium chloride (NaCl) to determine discharge (Q; Barbagelata, 1928; Day, 1976; Kilpatrick and Cobb, 1985) over mixing reach lengths of 12–50 m in the Bull Trout watershed and velocity–area gauging at the outlets of Stanley and Alturas Watersheds where dilution gauging was less appropriate. Each mixing reach length was determined with visual assessment using rhodamine-WT (Dingman, 2002). We calculated Q at each reach by dividing the injected mass by the integral of chloride concentration across the duration of the breakthrough curve (BTC).

Table I. Watershed summary statistics[a]

Watershed	Watershed area (km^2)	Network length (km)	Relief (m)	Drainage density
Alturas	62.8	75.4	1095	1.2
Stanley	33.0	47.8	1017	1.5
Yellowbelly	27.3	33.9	1090	1.2
Pettit	22.7	27.4	1054	1.2
Hellroaring	14.8	21.5	997	1.5
Bull Trout	11.4	14.4	466	1.3

Watershed	Median DFO (km)	Median LI (m^2/m)	Form factor	LI skewness
Alturas	8.9	0.25	0.59	6.8
Stanley	6.3	0.08	0.45	8.3
Yellowbelly	7.3	0.15	0.25	6.8
Pettit	5.8	0.21	0.33	7.0
Hellroaring	3.7	0.04	0.55	6.5
Bull Trout	3.4	0.20	0.27	6.1

[a] Summary statistics for the six study watersheds in the Sawtooth Mountains, ID, USA including stream network distance from outlet (DFO), lateral inflows (watershed contributing area) to a stream reach (LI), and Horton's (1932) form factor (area/straight-line basin length^2). Watershed outlet elevations range from 1988 to 2259 m with relief in the individual watersheds as listed.

We performed terrain analyses to determine watershed contributing area at every location where Q was measured. We quantified the relationship between watershed area and Q determined from synoptic discharge measurements on 24 July 2006 (Figure 1a; $r^2 = 0.82$). This synoptic sampling of discharge consisted of four dilution gauging measurements within the Bull Trout Watershed and velocity–area gauging at the outlets of the Stanley and Alturas Watersheds (Figure 1a, Table I). This relationship must be developed from synoptic data in order to characterize the relationship between area and Q under relatively instantaneous conditions. We quantified the relationship between Q and median tracer velocity across a range of observed flow states (~1–800 $L\,s^{-1}$) and stream sizes (first to third order) in ten different reaches in the Bull Trout watershed (see Covino *et al.*, 2011). We calculated median tracer velocity by dividing the reach length by the median of the tracer BTC arrival downstream. The median tracer velocity derived from observed BTCs includes contributions from advection and dispersion and thus partially incorporates both of these transport components into our estimates of network travel dynamics. The relationship between Q and median tracer velocity followed a power law function ($r^2 = 0.61$), consistent with findings by Calkins and Dunne (1970). Wondzell *et al.* (2007) compiled and reviewed the Q–velocity relationship derived from 241 other tracer tests performed across a broad range of watersheds and flow states (Figure 1b). Our local Q–velocity relationship fell well within this larger range of data (Wondzell *et al.*, 2007), providing a reference for how the watersheds used in this study relate to a broader set of watersheds. We implement these relationships in the development of the IW-VV-TTF (Figure 1).

Terrain analysis

We used a 1-m^2 resolution airborne laser swath mapping digital elevation model (DEM) product filtered to bare

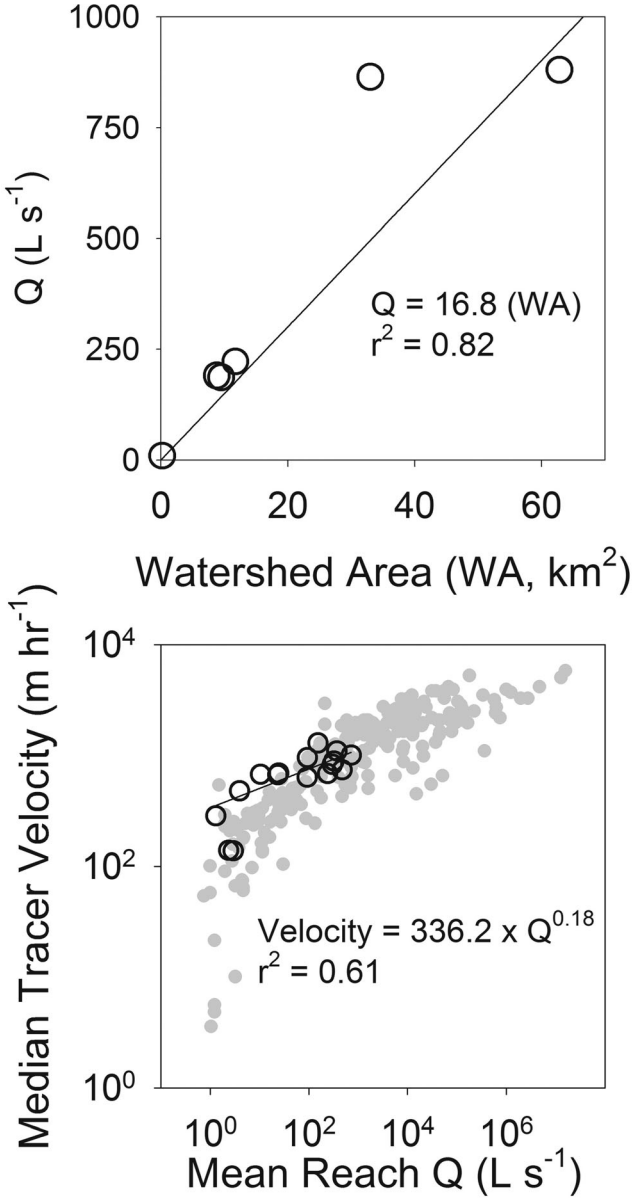

Figure 1. (a) Relationship between 24 July 2006 discharge (Q) and watershed contributing area based on empirical data from Bull Trout, Stanley, and Alturas watersheds. (b) Empirically derived relationship between discharge and velocity from 16 tracer tests performed in the Bull Trout Watershed (adapted from Covino *et al.*, 2011). Our data (black) show patterns similar to 241 tracer tests (grey) performed across a broad range of watersheds reviewed and compiled by Wondzell *et al.* (2007)

earth for the Bull Trout Watershed, collected and processed by the National Center for Airborne Laser Mapping. We resampled the DEM to 10 m by 10 m grid cell resolution for consistency with the other five watersheds analysed in this study. We acquired 10 m by 10 m grid cell resolution DEMs for the five remaining study watersheds from the United States Geological Survey (USGS) seamless server (data available from USGS, Earth Resources Observation and Science Center, Sioux Falls, SD). We preprocessed DEMs to remove sinks and dams (Olaya, 2004; Seibert and McGlynn, 2007) and clipped DEMs to each watershed boundary (with outlets just above or at the inlet of each watershed's terminal moraine lake) using a unidirectional flow direction algorithm (O'Callaghan and Mark, 1984). In order to objectively and simply compare watershed shape, we calculated Horton's (1932) form factor (Table I), which is watershed area divided by the square of straight-line basin length and characterizes a watershed's 'roundness'.

We calculated the watershed area, LIs, and stream network distances from outlet (DFO; the distribution of which is also known as the width function) for each stream cell in the study watersheds. We calculated the area contributing water to a particular watershed location, using a triangular multiple-flow direction algorithm (Jencso *et al.*, 2009; McGlynn and Seibert, 2003; Seibert and McGlynn, 2007) with a stream initiation threshold of 20 ha. This stream initiation threshold was assessed in the field as part of stream network mapping across the watersheds and deemed appropriate for these study sites. Watershed cells downstream of stream initiation locations were classified as stream cells, and area was routed using a single-direction flow algorithm (D8) (O'Callaghan and Mark, 1984; Seibert and McGlynn, 2007). If a stream cell flowed diagonally to the next we calculated DFO as sqrt (2) * 10 m to account for the extra distance from corner to corner of the cell. True stream DFOs could potentially be higher, especially in the more sinuous valley bottoms. The location and length of the true channel network is as accurate as possible using a 10-m DEM. LI at each stream cell (i.e. 10 m stream reach, Table I, Figure 2b) is the incremental increase in watershed area from one stream cell to the next in the downstream direction and represents the lateral watershed area that contributes water directly to a given stream cell (Jencso *et al.*, 2009; McGlynn and Seibert, 2003). The six study watersheds exhibited variable watershed structure and network geometry, including differences in hillslope length, drainage density, and watershed shape (Table I, Figure 2a). We analysed joint distributions of LI and DFO in conjunction with the empirical relationships between (1) watershed area and Q and (2) Q and velocity to derive IW-VV-TTFs for each watershed.

Travel time functions

We calculated IW-VV-TTFs for each watershed. They represent the distributions of stream network travel times from all locations of the stream network to the watershed outlet weighted by inflows (LI) to each stream cell. To calculate distributions of travel time, we first calculated travel time (T) through a given reach, r:

$$T_r = \frac{x_r}{u_r} \tag{1}$$

where x_r and u_r are length (in this study, a 10-m stream cell) and solute velocity at reach r, respectively. Velocity

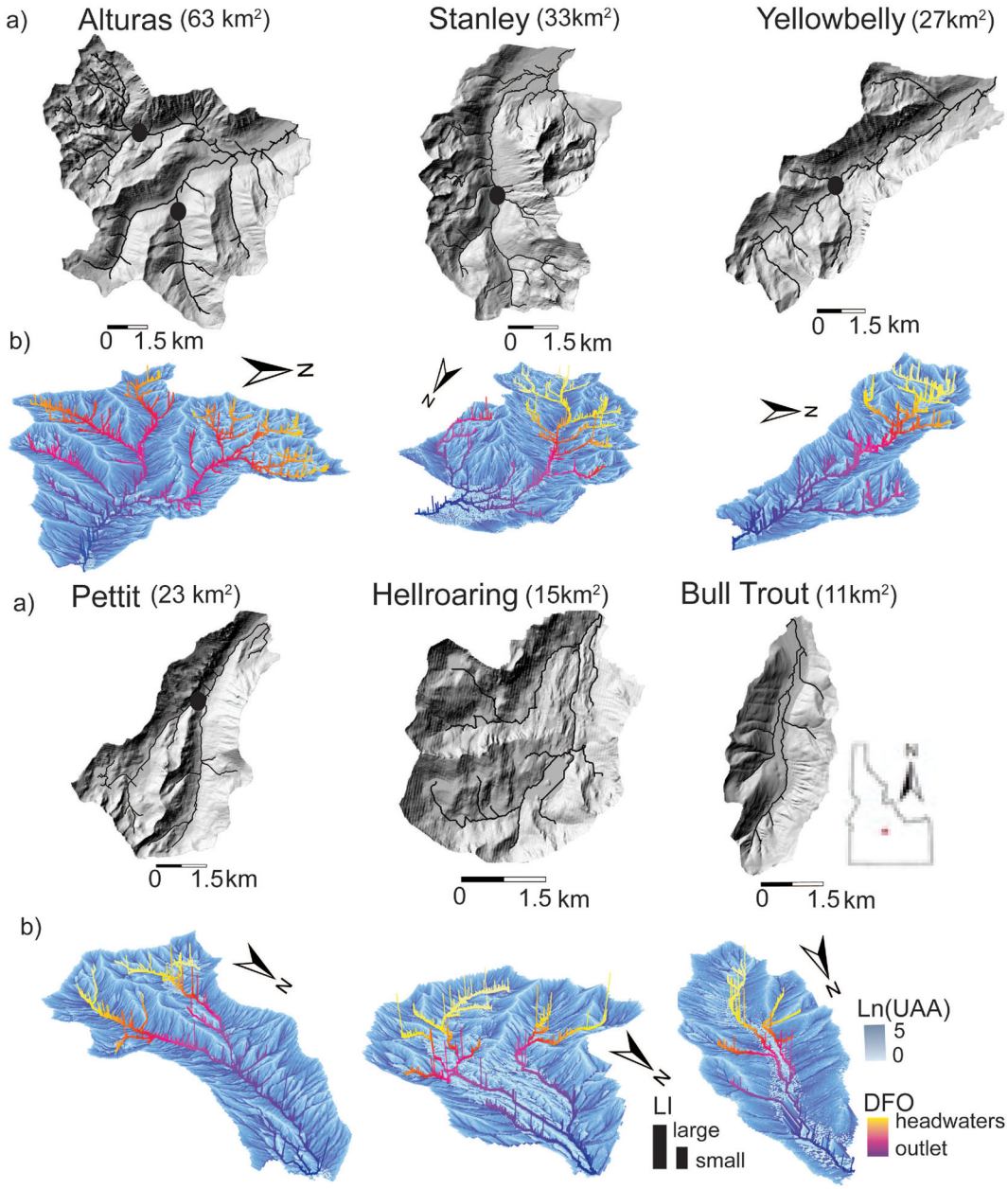

Figure 2. (a) Watersheds and stream networks displayed with hillshading to emphasize watershed shape and structure. Study location map at far right. (b) Upslope accumulated area superimposed on digital elevation models (DEMs) of each study watershed. Heights of bars along stream networks indicate magnitude of lateral inflow while bar colour indicates distance from watershed outlet. Points in the Alturas, Stanley, Yellowbelly, and Pettit watersheds indicate outlets of sub-watersheds used in analysis of the travel time function in watersheds of the same scale

in reach r is a function of discharge, established through the empirical relationship:

$$u_r = \alpha^* Q_r^{\beta} \tag{2}$$

where α and β are regression constants and Q_r is discharge in reach r. Q is calculated using the empirically estimated, linear relationship with contributing area:

$$Q_r = \gamma a_r \tag{3}$$

where a_r is total contributing area at reach r and γ is a regression constant. We substitute Equation 3 into Equation 2 to obtain velocity as a function of area.

$$u_r = \alpha(\gamma a_r)^{\beta} \tag{4}$$

To obtain the VV travel time function, Equation 4 is substituted into Equation 1 to obtain the travel time through a reach as a function of contributing area and reach length.

$$T_r = \frac{x_r}{\alpha(\gamma a_r)^{\beta}} \tag{5}$$

We calculate mean stream network velocity, $\bar{u}$, as the average of all u_r. We calculate the travel time function with a constant mean velocity (CV, IW-CV-TTF) for each stream network to highlight the influence of VV on travel time functions (Figure 3).

The total travel time from a given reach to the outlet, o, is the sum of all downstream T_r:

$$T_{r\to o} = \sum_{i=r}^{o} T_i = \sum_{i=r}^{o} \frac{x_i}{\alpha(\gamma a_i)^{\beta}} \tag{6}$$

where $T_{r\to o}$ is the travel time from reach r to the outlet. Once the travel time to the outlet for each reach is calculated, each travel time is weighted by the LI to the reach to estimate the proportional influence of a given travel time on the full travel time distribution. The inflow to a reach is equivalent to the incremental increase in discharge across the reach, which as shown in Equation 3 is a function of area. We weight all travel times:

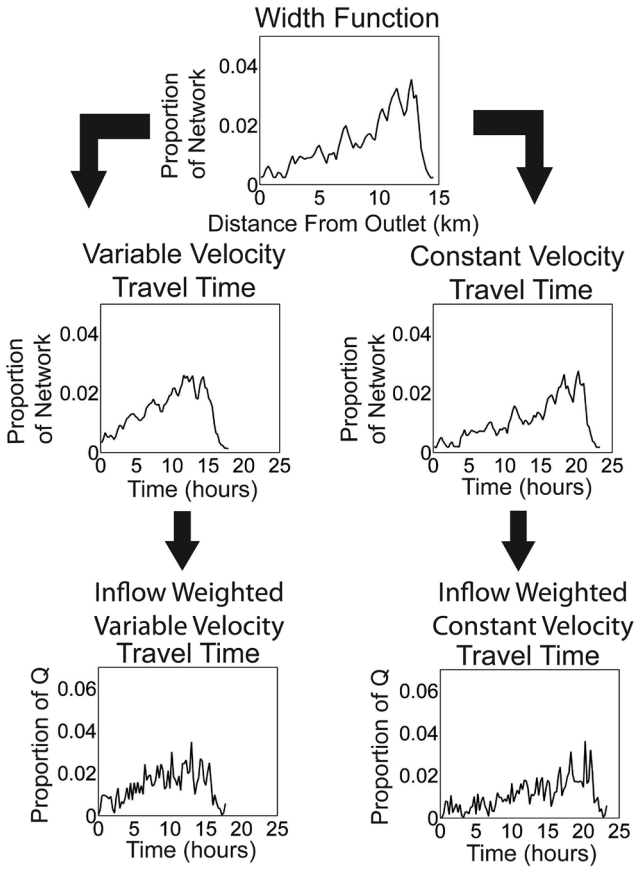

Figure 3. Flow chart describing the progression of components producing the variable velocity inflow weighted travel time function in Alturas watershed

$$\frac{1}{Q}\sum T_{r\to o}\, Q_{r\_\mathrm{LI}} = \overline{T} \tag{7}$$

where Q_{r_LI} is the LI for reach r (Figure 3). Summing the inflow or discharge weighted travel times and multiplying by $\frac{1}{Q}$, Q being the total discharge in the stream network, we determine the mean travel time ($\overline{T}$) for a given watershed. The distribution of all weighted travel times can be expressed as a probability distribution:

$$p\left(T_{r\to o}\,\frac{Q_{r\_\mathrm{LI}}}{Q}\right) \tag{8}$$

The IW-VV-TTF capitalizes on width function analyses and incorporates empirical relationships between flow and solute velocity to assess how watershed structure, the accumulation of streamflow, network geometry, and variable solute velocity influence travel time distributions across various watersheds.

RESULTS

The input weighted VV travel time function (IW-VV-TTF, Table A1) consists of several components calculated from watershed properties that are then progressively compiled. The development of the IW-VV-TTF and IW-CV-TTF (Figure 3) highlights the relative influence of each component and the differences between VV and CV in the resulting TTFs (Figure 3, Equations 1–8). The individual components and their compilation are described as follows.

Network geometry

The network geometries of each watershed produced unique width functions (Figure 4a). The Stanley Watershed width function approached a uniform distribution because of its more linear stream network with roughly equivalent proportions of stream reaches at each distance. Yellowbelly and Bull Trout are the most elongated, as indicated by the form factors 0.25 and 0.27, respectively (Table I). Despite similarities in shape between Bull Trout and Yellowbelly, they have different stream network configurations and therefore different width functions, but both have more variable distributions of DFO than the Stanley watershed. The Bull Trout width function has a large peak (Figure 4a) with a greater proportion of the stream network located between 3 and 5 km from the watershed outlet. This is the result of two nearly parallel channels and the presence of first-order tributaries along those reaches. Yellowbelly has a more uniform distribution because it has a single main channel fed mostly by small first-order streams. Despite its relatively small size

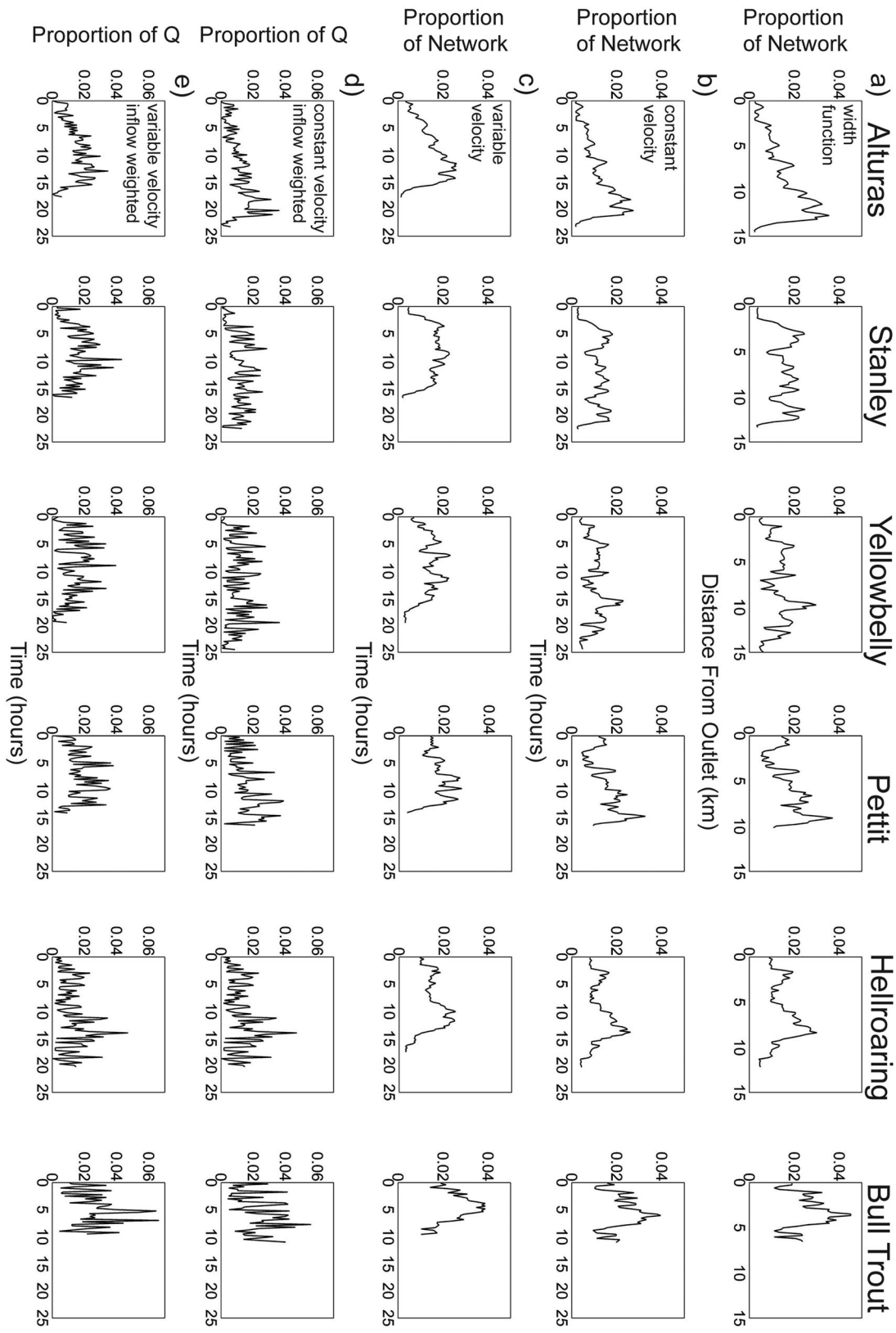

Figure 4. Progression (vertically) of the calculated travel time function for all six study watersheds (horizontally). The basis of the travel time function is the distribution of network distances (the width function) (a). Travel time can be calculated with a constant velocity (b) or a variable velocity (c). The travel times can be weighted by lateral inflows to the stream network (d). When all pieces are incorporated, the result is the inflow weighted variable velocity travel time function (e) presented as proportion of total discharge (Q) in the network at a given time

(27.3 km^2, I1), Yellowbelly has the longest channel network, 0.6 km longer than the much larger but more round Alturas Watershed (area 62.8 km^2, form factor 0.59, Table I). The width function in the highly bifurcated Alturas Watershed follows a quasi-exponential pattern because of the higher proportion of stream reaches farther from the outlet and a median DFO much greater than all other watersheds (Table I). Stream network geometries play important roles in the travel time distributions because they directly relate to the distances water must travel to the watershed outlet, the locations of upland contributions to streamflow, and the pattern and magnitude of velocity change downstream.

If one assumes a CV, the width function can serve as a first approximation of network travel times (Kirkby, 1976). In this case, the travel time function would mirror the width function shape but would be rescaled by the singular transport velocity (Moussa, 2008; Figure 4a, b). Here, we calculated the CV travel time function using stream network mean velocity and applied it to the width functions (Figure 4b). The subsequent two additions to the TTF (VV and inflow weighting) each affected the final TTF in different ways; for illustration we calculated the distribution of travel times considering each component separately (Figure 3).

Velocity approximations

The VV travel times were faster than the CV travel times in all study watersheds (Table II, Figure 4b, c, Equation 5). In each watershed, there were proportionally more small headwater stream reaches with low Q and velocity than reaches with higher discharge and velocity on the main stems of the watersheds. This caused mean stream network velocity to be skewed towards lower velocities and resulting mean CV travel times to be considerably longer. The travel time distributions shifted with the introduction of VV. Although general shapes were preserved, locations and magnitudes of peaks in these distributions were not equivalent. Peaks were muted and troughs were less pronounced in all watersheds under VV. This was particularly evident in the Alturas and Stanley Watersheds. In the Stanley Watershed, VV introduced a 'smoothing and compressing' effect on the peaks in the width function (Figure 4c).

The spatial distribution of velocity is influenced by the rate of cumulative increase in contributing area (because of its influence on Q) along the stream network from headwaters to the watershed outlet. The Pettit and Hellroaring watersheds facilitate direct comparison of how variable watershed structure and network geometry can affect velocity and resulting travel time distributions. Hellroaring is a small, round watershed (form factor of 0.55) with a highly dendritic stream network. Pettit is a linear watershed (form factor of 0.33) drained by two channels converging to a main channel in the lower third of the watershed (Figure 2). Because of the nature of these watershed structures, Hellroaring has a drainage density considerably higher than the Pettit Watershed, 1.5 *versus* 1.2 (Table I). In fact, Hellroaring has a substantially higher drainage density than the other five study watersheds and the lowest median LI, partially attributable to the high drainage density. Within the range studied here, larger watersheds will have greater discharge and exhibit higher final velocities (velocity at the watershed outlet, Figure 1, Equations 2 and 3). Pettit exhibited a higher final velocity because it is about 1.5 times larger than Hellroaring. However, network travel times are controlled by the velocities through the entire stream network, and it is here where the internal structure of the watershed becomes important: velocities increase more gradually in Hellroaring than in Pettit because smaller LIs are distributed more evenly across more stream network of the Hellroaring Watershed (Table I). Pettit has a stream network 5.9 km longer than Hellroaring, but despite this disparity in length we calculate maximum travel times in Pettit that are 3.4 h faster than in Hellroaring (Table II, max TT) because flow is concentrated in fewer channels, and therefore, velocity is greater (Figures 2 and 4). The Pettit and Hellroaring watersheds exemplify how different watershed structure and network geometry can affect the incremental increase in solute transport velocity through the stream network and strongly influence resulting travel time distributions.

Table II. Watershed travel times[a]

	Alturas		Stanley		Yellowbelly		Pettit		Hellroaring		Bull Trout	
Watershed	CV	VV	CV	VV	CV	VV	CV	VV	CV	VV	CV	VV
Mean IWTT (h)	14.3	9.8	12.6	8.9	12.6	9.2	9.8	7.5	11.3	9.5	6.3	5.2
Max IWTT (h)	23.4	18.0	22.7	17.0	24.5	19.7	16.7	14.3	20.5	17.6	11.2	9.7
Skewness	−0.66	−0.40	−0.02	0.01	−0.09	0.05	−0.48	−0.20	−0.20	−0.13	0.05	0.12

[a] Mean and maximum inflow weighted travel time (IWTT) in hours and skewness of each watershed calculated using both and constant and variable velocity (CV and VV, respectively).

Inflow weighting

Inflow weighting, necessitated by heterogeneous spatial patterns of water delivery to the stream network (LI, height of bars in Figure 2b), is determined by the topographically driven redistribution of water in the uplands as illustrated with patterns of how total watershed area accumulates along the stream network in Figure 2b. Variable LIs are not only key for inflow weighting but when combined with network geometry they dictate change in velocity from one reach to the next and the resulting travel times across the stream network. The distributions of LI were highly skewed towards small LIs (Figure 2b). Calculated skewness (i.e. the third statistical moment of a distribution) of LI ranged from a minimum of 6.13 in Bull Trout up to 8.28 in the Hellroaring Watershed. Larger and often strongly convergent hillslopes, although less frequent, provided much larger inflows to the stream network (up to a maximum LI of 42.4 ha in Yellowbelly Watershed). The inflow weighting, even with a CV travel time function, changed the shapes of the original width functions of the stream networks (Figure 4d). The locations and frequency of peaks in the non-IW distributions (Figure 4b, c) were altered in the IW distributions (Figure 4d, e) with the inflow weighting leading to greater numbers of peaks and troughs in the distributions.

The combination of inflow weighting and VV generates travel time distributions that reflect the spatial intersection of the distributions in Figure 4c, d. The peakedness of the inflow weighting was still prominent in the final IW-VV-TTFs while the smoothing and compressing effect of VV was also discernable. In the Alturas Watershed, the influence of the high proportion of headwaters streams (Figure 4a) decreased in the final TTF (Figure 4e). The peak observed at 9 km in the Pettit stream network width function (Figure 4a) became muted and of smaller relative magnitude than other peaks in the VV travel time function (Figure 4c) but did persist to the final IW-VV-TTF (Figure 4e).

In the full IW-VV-TTF, at a given DFO, there can be multiple inputs with different travel times. In highly dendritic channel networks, or a specific location where multiple channels are at roughly the same distance from the watershed outlet (peaks in width functions, Figure 4a), various hillslope sizes will be contributing water to each channel, and the inputs will be made to various downstream velocity conditions, resulting in variable travel times. This is best illustrated in Figure 5, where travel time is a third variable represented by the colour scale across the distribution of LIs over the stream network of all six study watersheds. The inset of the Hellroaring Watershed LI and TT distribution at 3 to 7 km DFO illustrates how there can be large differences in travel time for a given DFO. Each watershed not only has a unique overall travel time function (Figure 4e) but also has a unique makeup of contributing areas and travel times throughout the watershed within the travel time function (Figure 5).

Watershed scaling

Although the original six watersheds are of relatively similar size (Table I), the travel times varied as a function of watershed and stream network size. Therefore, we selected sub-watersheds that were within 3 km^2 of the Bull Trout watershed area (~11 km^2, Figure 6) and compared their IW-VV-TTFs. Outlets of sub-watersheds within the original study watersheds are indicated as points on the stream networks in Figure 2. The areas of the sub-watersheds range from 8.24 to 12.67 km^2. The Stanley sub-watershed was more round and had a dendritic drainage pattern while Alturas left tributary sub-watershed was similarly round, but with two main channels converging directly before the watershed outlet (Figure 6a, b). Conversely, the Bull Trout and Alturas right tributary sub-watershed were relatively linear (elongated) in shape. Despite their differences in watershed shape and resulting network geometry, all six stream network mean travel times were within ~40 min of each other (4.11–4.77 h), and maximum travel times were also within a few hours of each other. Overall, the same scale watershed comparisons exemplify how varying watershed structure and resultant LI heterogeneity can influence the final stream network IW-VV-TTF and thereby the amount of time (distribution of times) it takes solutes and water molecules to travel through the stream network.

DISCUSSION

We present analysis of how watershed structure and stream network geometry can affect solute travel times and discuss implications for interpreting observed watershed outflow signatures. We developed an IW-VV-TTF that represents the probability distribution of conservative solute travel times, as a surrogate for the water molecules themselves, from entry into the stream network to a given watershed outlet. The IW-VV-TTF builds on the commonly used width function and combines direct measures of watershed structure, stream network geometry, and solute velocity to estimate stream network travel time distributions.

Network geometry sets the distribution of travel distances for water and solutes from entry to the stream network to the watershed outlet and therefore is a first-order control, or the basic template for stream network travel times. This routing affects the timing of arrival from different spatial sources independent of transport velocities (Figures 2, 4a, b, 5) and is illustrated by the

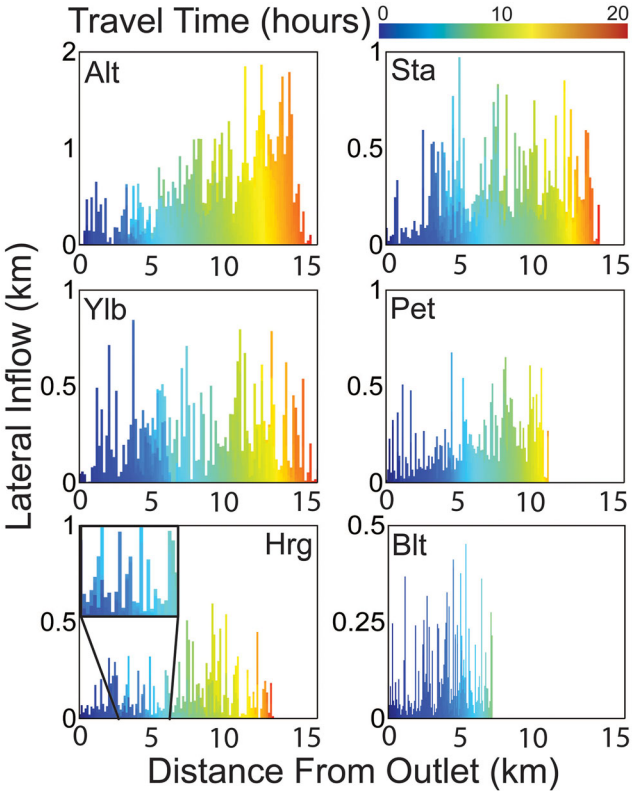

Figure 5. Distributions of lateral upland water contributions (bar height) and travel times (colour scale) over the range of stream network travel distances (*x*-axis) in the Alt (Alturas), Blt (Bull Trout), Hrg (Hellroaring), Pet (Pettit), Sta (Stanley), and Ylb (Yellowbelly) watersheds. Multiple lateral inputs contributing at a given distance from the outlet can have different travel times as indicated by bars composed of multiple colours and demonstrated in the inset in the Hrg watershed. Note rescaled *y*-axes for Alt and Blt.

shape of the width function (Figure 4a and 5b). However, its utility can be limited in cases where the average velocity is unknown, the variation in velocities is substantial, and where LIs or weighting of inflows at different distances are not considered.

For a given DFO and flow state, there exists a range of stream network travel times to the watershed outlet. A small first-order stream reach and a reach of the main stem of a stream network could have the same LI magnitude and network travel distance; however, because of different downstream distributions of velocities, the inflows to these reaches could have very different travel times to the watershed outlet (Figure 5). Naturally then, because of velocity differences, a given travel time consists of water from different travel distances. The initial velocity for an inflow to the stream network is a function of the integrated upstream LIs or total upstream catchment area (proportional to Q and therefore velocity), while a particle of water's future velocity is a function of downstream-accumulated LIs, or increases in watershed area, discharge, and velocity. Understanding this variation of in-stream network transport times for a given particle of water and associated solutes can provide insight into its exposure to in-stream biological processes (e.g. Lindgren and Destouni, 2004) and potential for exchange with sediments (e.g. Gupta and Cvetkovic, 2002).

These observations illustrate that a solute signature or parameter observed at the watershed outlet is composed of water and solutes that have come from source areas heterogeneously distributed across the stream network. For example, even in the modestly sized, relatively similar watersheds presented here, there were up to 2.6 km differences in distance travelled to the outlet for inflows with the same travel time and up to 3.1 h differences in travel time for inflows with the same travel distance. These differences would increase with both increasing basin size and more variable morphology and network configurations. This can have strong implications for solute transport and the degree of nutrient removal in downstream flow (Wollheim *et al.*, 2006). For example, Mineau *et al.* (2015) demonstrated that within a network scale nutrient removal model, nutrients loaded in the headwaters had a twofold increase in removal relative to those closer to the outlet. They attributed this to longer travel times and slower velocities in the headwaters, amongst other processes.

Variable velocity, LIs and resulting travel time through a stream network can have significant ramifications for interpreting solute dynamics such as nutrients (Heffernan and Cohen, 2010) and metals (Nimick *et al.*, 2011) or for using their daily amplitude to infer or quantify process rates. Because of potentially wide ranging travel times between LIs and downstream sampling locations, signals can be muted or amplified because of destructive or constructive interference respectively (Wondzell *et al.*, 2010). Fonely *et al.* (2015) tested this theory of signal interference proposed by Wondzell *et al.* (2010). They demonstrated using stream order dependent velocity, signals such as diel discharge can be dampened because of travel time integration. Although gas transfer influences diel dissolved oxygen (Mullholland *et al.*, 2005) and carbon dioxide dynamics, this method can be useful in comparing watershed *versus* reach scale signals. For example, a two-station stream metabolism approach coupled with the IW-VV-TTF could be particularly useful for understanding how reach scale biogeochemical and metabolic processes scale up to the watershed level. Alteration of biogeochemical signals travelling through the system will be partially dependent on network geometry and watershed structure (e.g. Figures 4 and 6). Therefore, interpretation of in-stream solute (e.g. nutrient) and gas (e.g. dissolved oxygen) dynamics necessitates estimation or at least appreciation of variable travel distances and times and their potential impact on observed signatures.

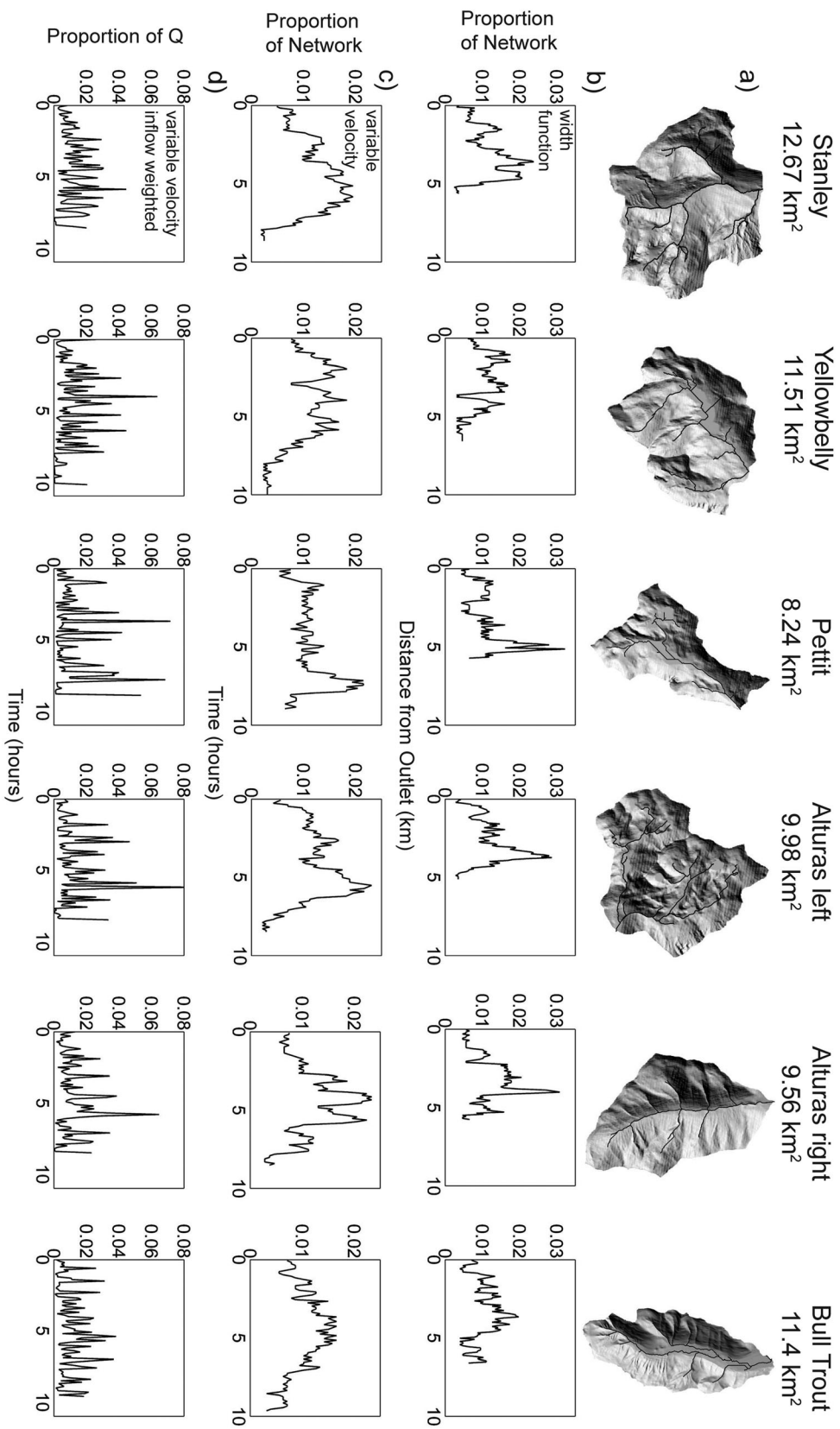

Figure 6. Travel time calculations for study sub-watersheds comparable in area to the Bull Trout watershed. Each watershed's morphology (a) produce respective width functions, (b) variable velocity travel time functions (c), and inflow weighted variable velocity travel time functions (d) as proportion of total network discharge (Q).

Here we calculated variable solute velocity across the stream network from an empirical relationship between median tracer velocity and discharge developed from 16 tracer experiments across a wide range of flow conditions and channel sizes (Figure 1b). This empirical relationship allows us to assign a unique velocity as a function of discharge in each stream cell of each network. We used the median tracer velocity, derived from observed BTCs, from our tracer tests as a characteristic metric of the full range of transport velocities we observed. Other velocity metrics could be chosen to accentuate one or another transport component more heavily. For instance, a modal velocity (time to BTC peak) could be used to assess advective transport and the role of network geometry in attenuating advective pulses. Alternatively, a velocity developed from the time to tracer departure (e.g. 95% tracer arrival, sensu Runkel, 2015) could be used to assess the slow (BTC tail) component of transport. Therefore, metrics such as modal, mean, median, and departure velocities could be used to determine upper and lower limits along with more average transport behaviour. Here we have used the median velocity for simplicity and for consistency with the tracer/solute velocity review of Wondzell (2007).

Velocity metrics that more strongly emphasize dispersion (e.g. departure velocity) would elongate travel times, particularly in headwater locations. Our experimental data indicate greater BTC tailing behaviour in headwater compared with higher order (e.g. valley bottom) stream reaches (see Covino *et al.*, 2011). This pattern has been observed in other studies and is partially due to lower discharge and the higher proportion of water exchanged with the streambed in headwater locations (Haggerty *et al.*, 2002). Depending on the process of interest, different solute velocity metrics may be more or less appropriate. For instance, the departure velocity could be useful for assessing biogeochemical processes that have very slow kinetics or to estimate the upper bound on pollutant and contaminant travel times. Conversely, a modal travel velocity (i.e. dominated by advection) could be useful for estimating maximum downstream concentrations of a nutrient, pollutant, or contaminant. In addition to these different solute velocities, longer spatial and temporal scale groundwater–surface water exchange of water and solutes (i.e. hydrologic turnover; Covino *et al.*, 2011; Covino and McGlynn, 2007; Mallard *et al.*, 2014; Payn *et al.*, 2009) has not been accounted for here but would additionally influence stream water solute signatures. While it could be possible to incorporate transport phenomena such as transient storage, hydrologic turnover, and dispersion more explicitly, we chose median tracer velocity as a concise representation of advection, dispersion, transient storage, and turnover in order to focus on the specific effects of network geometry, variable solute velocities, and weighting by variable sources.

We have demonstrated differences in water and solute travel time estimates as a function of different velocity calculations (CV and VV) as exemplified by shifting shapes of the TTFs (Figure 4) and changes in the mean, median, and skew of the frequency distributions (Table II). Other studies have employed a variety of strategies to address in-stream network transport. Some have used velocities derived from hydraulic geometry relationships (Alexander *et al.*, 2002; Darracq *et al.*, 2010) for solute transport time estimates, while others have used the velocity calculated from Manning's equation (e.g. Worrall *et al.*, 2013). It should be noted that hydraulic geometry and Manning's equation calculated velocities are not equivalent to solute transport velocities estimated from tracer tests and that hydraulic geometry derived velocity estimates are typically much greater (i.e. faster). In some studies, a single value of velocity is applied across an entire network. When we applied the IW-VV-TTF to the similar-sized smaller watersheds, we found that the shapes of the travel time distributions and locations, numbers, and magnitudes of peaks were variable across networks (Figure 6c, d). This suggests that using a basin average travel time (e.g. Worrall *et al.*, 2014) is not sufficient to understand in-stream processes or the range and frequency of travel times that can vary strongly within a network or from one network to the next.

Experimentally derived solute transport velocities, like the one employed in our study, have also been used by others (e.g. Wondzell *et al.*, 2007). Extrapolation of these derived velocities to longer stream reaches, other reaches, and whole stream networks has been approached in numerous ways, such as over Strahler orders, (e.g. Saco and Kumar, 2002a; Fonley *et al.*, 2015) or constant in space but variable in time (e.g. Valdes *et al.*, 1979). Each of these approaches will result in different approximations of network velocity. Unfortunately, we are not aware of any universal relationship between kinematic velocity and solute velocity because of the reality of heterogeneity and exchange in natural systems. Therefore, the conversion between a hydraulic geometry based velocity estimate such as kinematic or Manning's type and solute transport velocity remains a challenge. We suggest that studies carefully consider what estimate of velocity is most appropriate for their questions or needed for adequate data interpretation. In the absence of site-specific information, the global relationship described by Wondzell *et al.* (2007) could be useful in translating Q variability across networks into likely water particle and solute velocity within reaches and then scaled across networks.

In addition to the influences of VV and network geometry on travel time distributions, it is also valuable to consider the magnitude of the inflows along the stream

network and their proportional influence on downstream observations (Figure 5). It has been acknowledged that across a given watershed, hillslopes have variable shape (topography), which influences the magnitude of inputs to streams (Anderson and Burt, 1978; Jencso *et al.*, 2009). Here we employ a proportional LI for simplicity. However, the work of Jencso *et al.* (2009) suggests that over dynamic flow conditions, saturated hillslope throughflow exhibits threshold behaviour as a function of hillslope size. This could lead to nonlinear relationships between watershed area and LI or stream discharge at fine spatial scales and represents a hydrological process that also should be considered in interpretation of observed outlet signals. Threshold mediated saturated connectivity of uplands and streams could provide a valuable complement to this study because the work presented here is focused on the routing of hillslope inflows through stream networks rather than any upland processes *per se*.

Should these principals be applied across changing flow states (rather than at baseflow such as in this study), the temporally variable contribution of hillslopes could additionally obscure or confound observed outlet signals. Future research could include threshold mediation of hillslope throughflow contributions to streamflow and subsequent IW-VV-TTF calculated dynamically across variable flow conditions. In a review of studies taking a geomorphologic approach to estimating travel times, Gupta and Mesa (1988) state that variable terrestrial inflows along a stream network are sometimes excluded from analyses. In our study, we found that inflow weighting produced a pronounced effect on the proportion of discharge arriving at the watershed outlet for a given travel time (Figures 4 and 5) and is likely an important consideration.

Stream network travel times are just one component of whole watershed travel times that are themselves the focus of much past and ongoing research (e.g. Benettin *et al.*, 2013a, b, 2015; Harman, 2015; Heidbuchel *et al.*, 2012; Kirchner *et al.*, 2001; McGuire and McDonnell, 2006; Rinaldo *et al.*, 2011). As such, stream network IW-VV-TTFs could provide insight into the role of the channel network as a final 'temporal filter' on water leaving watersheds. More comprehensive understanding of the relative roles of different portions of the landscape in contributing to full watershed travel time distributions represents a grand challenge in hydrology. Approximating stream network travel time distributions therefore represents a first step towards parsing landscape element influences on whole watershed travel time distributions.

These analyses could be extended to any watershed where drainage is topographically controlled or other information on the spatial pattern of lateral or groundwater inflows to the stream network can be estimated. Spatial data sets of sufficient resolution are readily available (e.g. DEMs) for virtually any watershed. The terrain analysis used to quantify network structure and LIs for weighting utilized well-established methods. Our modelled estimates of discharge and velocity required iterative application of simple equations across the stream network. In this study, we exploited the locally measured transport velocities (Figure 1b, black open circles), corroborated by the global (Figure 1b, grey dots; *Wondzell et al.*, 2007) relationship between streamflow magnitude and tracer velocity. The generalized relationship synthesized from a wide range of streams, flow states, and physiographic regions presented by Wondzell *et al.* (2007) could be used where local information is unavailable. These relationships were best fit by a power law; however, they could overestimate discharge at low velocities. As the travel time function is applied to larger watersheds, the overestimation of velocity and resulting underestimation of travel time would be reduced, and travel time estimates would be improved. We also recognize that other empirical relationships using morphometric or hydrologic parameters may be more reasonable or more readily measured in other watersheds. Regardless of the method selected, the overall approach is widely applicable and easily implemented and could readily inform network travel time estimates and stream observation interpretation.

CONCLUSION

We developed IW-VV-TTFs for six watersheds of differing sizes and structures but with similar climatological forcing, land cover, and landscape evolution histories. We documented variable travel time distributions that indicated differential network filtering of baseflow watershed runoff signatures across these seemingly similar catchments. Examination of the IW-VV-TTFs helped elucidate the relative influences of watershed structure, network geometry, and VV in organizing and filtering signals observed along stream networks. These components: upland watershed structure, stream network geometry, and VV have been considered in various forms and combinations in a range of studies, particularly in rainfall–runoff response modelling. We have outlined how the factors can be adapted and combined, particularly with the use of a variable solute velocity, to inform observations and studies focused on the transport of water and solutes under baseflow conditions. This integrative approach indicates that inflow weighting, variable solute velocity, and network geometry are fundamental to the distribution of stream network travel times and could be used to help interpret watershed outlet observations as a function of their constituent spatial and temporal causal processes.

ACKNOWLEDGEMENTS

Financial support was provided by grants from the National Science Foundation to McGlynn (DEB-0519264 and EAR-0837937), an Environmental Protection Agency (EPA) STAR Fellowship awarded to Covino, and a Montana State University Undergraduate Scholars Program award to Bergstrom. We would like to thank Brian Iacona, Kelly Conde, Malcolm Herstand, and Alexey Kalinin for assistance with fieldwork and the Boise National Forest for allowing access to sampling sites.

REFERENCES

Agnese C, Dasaro F, Giordano G. 1988. Estimation of the time scale of the geomorphologic instantaneous unit-hydrograph from the effective streamflow velocity. *Water Resources Research* **24**(7): 969–978. DOI:10.1029/WR024i007p00969.

Alexander RB, Elliott AH, Shankar U, McBride GB. 2002. Estimating the sources and transport of nutrients in the Waikato River Basin, New Zealand. *Water Resources Research* **38**(12):. DOI:10.1029/2001WR000878.

Anderson M, Burt T. 1978. Role of topography in controlling throughflow generation. *Earth Surface Processes and Landforms* **3**(4): 331–344. DOI:10.1002/esp.3290030402.

Barbagelata A. 1928. Chemical–electrical measurement of water. *American Society of Civil Engineers Proceedings* **54**: 789–802.

Benettin P, van der Velde Y, van der Zee SEATM, Rinaldo A, Botter G. 2013a. Chloride circulation in a lowland catchment and the formulation of transport by travel time distributions. *Water Resources Research* **49**: 4619–4632.

Benettin P, Rinaldo A, Botter G. 2013b. Kinematics of age mixing in advection–dispersion models. *Water Resources Research* **49**: 8539–8551.

Benettin P, Kirchner JW, Rinaldo A, Botter G. 2015. Modeling chloride transport using travel time distributions at Plynlimon, Wales. *Water Resources Research* **51**: 3259–3276. DOI:10.1002/2014WR016600.

Beven KJ. 1978. The hydrological response of headwater and sideslope areas. *Hydrological Sciences Bulletin* **23**(4): 419–437.

Beven KJ, Wood EF, Sivapalan M. 1988. On hydrological heterogeneity —catchment morphology and catchment response. *Journal of Hydrology* **100**: 353–375.

Calkins D, Dunne T. 1970. A salt tracing method for measuring channel velocities in small mountain streams. *Journal of Hydrology* **11**(4): 379–392.

Covino T, McGlynn B. 2007. Stream gains and losses across a mountain-to-valley transition: impacts on watershed hydrology and stream water chemistry. *Water Resources Research* **43**:. DOI:10.1029/2006WR005544.

Covino T, McGlynn B, Mallard J. 2011. Stream–groundwater exchange and hydrologic turnover at the network scale. *Water Resources Research*. DOI:10.1029/2011WR010942.

Darracq A, Destouni G, Persson K, Prieto C, Jarsjo J. 2010. Quantification of advective solute travel times and mass transport through hydrological catchments. *Environmental Fluid Mechanics* **10**: 103–120. DOI:10.1007/s10652-009-9147-2.

Day TJ. 1976. Precision of salt dilution gauging. *Journal of Hydrology* **31**(3-4): 293–306. DOI:10.1016/0022-1694(76)90130-X.

Dingman SL. 2002. *Physical Hydrology, Appendix F*. Prentice Hall: Upper Saddle River, N.J.

Fonley M, Mantilla R, Small SJ, Curtu R. 2015. On the propagation of diel signals in river networks using analytic solutions of flow equations. *Hydrology and Earth System Sciences Discussions* **12**: 8175–8220. DOI:10.5194/hessd-12-8175-2015.

Funkhouser JE, Barks CS. 2004. Development of a travel time prediction equation for streams in Arkansas, U.S. Geological Survey Investigations Report, 2004-5064.

Graf JB. 1995. Measured and predicted velocity and longitudinal dispersion at steady and unsteady flow, Colorado River, Glen Canyon dam to Lake Mead. *Water Resources Bulletn American Water Resources Association* **31**(2): 265–281.

Gupta A, Cvetkovic V. 2002. Material transport from different sources in a network of streams through a catchment. *Water Resources Research* **38**(7):. DOI:10.1029/2000WR000064.

Gupta V, Mesa OJ. 1988. Runoff generation and hydrologic response via channel network geomorphology—recent progress and open problems. *Journal of Hydrology* **102**: 3–28.

Gupta V, Waymire E. 1983. On the formulation of an analytical approach to hydrologic response and similarity at the basin scale. *Journal of Hydrology* **65**(1–3): 95–123. DOI:10.1016/0022-1694(83)90212-3.

Gupta V, Waymire E, Wang C. 1980. A representation of an instantaneous unit-hydrograph from geomorphology. *Water Resources Research* **16**(5): 855–862. DOI:10.1029/WR016i005p00855.

Haggerty R, Wondzell SM, Johnson MA. 2002. Power-law residence time distribution in the hyporheic zone of a 2nd-order mountain stream. *Geophysical Research Letters* **29**(13):. DOI:10.1029/2002GL014743.

Harman CJ. 2015. Time-variable transit time distributions and transport: theory and application to storage-dependent transport of chloride in a watershed. *Water Resources Research* **51**: 1–30. DOI:10.1002/2014WR015707.

Heffernan JB, Cohen MJ. 2010. Direct and indirect coupling of primary production and diel nitrate dynamics in a subtropical spring-fed river. *Limnology and Oceanography* **55**(2): 677–688.

Heidbuchel I, Troch PA, Lyon SW, Weiler M. 2012. The master transit time distribution of variable flow systems. *Water Resources Research* **48**: W06520. DOI:10.1029/2011WR011293.

Horton R. 1932. Drainage-basin characteristics. *Transactions-AGU* **13**: 350–361.

Jencso K, McGlynn B, Gooseff M, Wondzell S, Bencala K, Marshall L. 2009. Hydrologic connectivity between landscapes and streams: transferring reach-and plot-scale understanding to the catchment scale. *Water Resources Research* **45**: W04428. DOI:10.1029/2008WR007225.

Jobson HE (1996), Prediction of travel time and longitudinal dispersion in rivers and streams. U.S. Geological Survey Water Resources Investigations Report 96-4013.

Kiilsgaard T, Stanford L, Lewis R. 2003. Preliminary geologic map of the northeast part of the Deadwood River 30 × 60 minute quadrangle, Idaho, Idaho Geologic Survey.

Kilpatrick FA, Cobb ED. 1985. Measurement of discharge using tracers, *Report of the U.S. Geological Survey*, *Techniques of Water Resources Investigations*, Book 3, Chap. A16, U.S. Geol. Survey.

Kirchner JW, Feng X, Neal C. 2001. Catchment-scale advection and dispersion as a mechanism for fractal scaling in stream tracer concentrations. *Journal of Hydrology* **254**: 82–101.

Kirkby M. 1976. Tests of random network model, and its application to basin hydrology. *Earth Surface Processes Landforms* **1**(3): 197–212. DOI:10.1002/esp.3290010302.

Kirkby M, Chorley RJ. 1967. Throughflow, overland flow and erosion. *Internation Association Scientific Hydrology Bulletin* **12**(3): 5–21.

Lashermes B, Foufoula-Georgiou E. 2007. Area and width functions of river networks: new results on multifractal properties. *Water Resources Research* **43**: W09405. DOI:10.1029/2006WR005329.

Lee K, Yen B. 1997. Unit hydrograph derivation for ungauged watersheds by stream-order laws. *Journal of Hydrologic Engineering* **2**(1): 1–9. DOI:10.1061/(ASCE)1084-0699(1997)2:1(1).

Leopold L. 1953. Downstream change of velocity in rivers. *American Journal of Science* **251**(8): 606–624.

Leopold, L, and Maddock T (1953), The hydraulic geometry of stream channels and some physiographic implications, *U.S. Geol. Surv. Prof. Pap.*, 282-A.

Leopold L, Wolman M, Miller J. 1964. *Fluvial Processes in Geomorphology*. Dover Publications: New York; 242–248.

Lightbill MJ, Whitham GB. 1955. On kinematic waves: flood movement in long rivers. *Proceedings Royal Society (London) Series A* **229**: 281–316.

Lindgren GA, Destouni G. 2004. Nitrogen loss rates in streams: scale-dependance and up-scaling methodology. *Geophysical Research Letters* **31**: L13501. DOI:10.1029/2004GL019996.

Luhmann AJ, Covington MD, Alexander SC, Chai SY, Schwartz BF, Groten JT, Alexander ECA Jr. 2012. Comparing conservative and nonconservative tracers in karst and using them to estimate flow path geometry. *Journal of Hydrology* **448-449**: 201–211. DOI:10.1016/j.jhydrol.2012.04.044.

Mallard JM, McGlynn B, Covino TP. 2014. Lateral inflows, stream-groundwater exchange, and network geometry influence streamwater composition. *Water Resources Research*. DOI:10.1002/2013WR014944.

McDonnell JJ, Beven K. 2014. Debates—the future of hydrological sciences: a (common) path forward? A call to action aimed at understanding velocities, celerities, and residence time distributions of the headwater hydrograph. *Water Resources Research* **50**: 5342–5350. DOI:10.1002/2013WR015141.

McGlynn B, Seibert J. 2003. Distributed assessment of contributing area and riparian buffering along stream networks. *Water Resources Research* **36**(4):. DOI:10.1029/2002WR001521.

McGuire KJ, McDonnell JJ. 2006. A review and evaluation of catchment residence time modeling. *Journal of Hydrology* **330**: 543–563. DOI:10.1016/j.jhydrol.2006.04.020.

Mineau MM, Wollheim WM, Stewart RJ. 2015. An index to characterize the spatial distribution of land use within watersheds and implications for river network nutrient removal and export. *Geophysical Research Letters* **42**:. DOI:10.1002/2015GL064965.

Moussa R. 2008. Effect of channel network topology, basin segmentation and rainfall spatial distribution on the GIUH transfer function. *Hydrological Processes* **22**: 395–419.

Mullholland PJ, Houser JN, Maloney KO. 2005. Stream diurnal dissolved oxygen profiles as indicators of in-stream metabolism and disturbance effects: Fort Benning as a case study. *Ecological Indicators* **5**: 243–252. DOI:10.1016/j.ecolind.2005.03.004.

Nimick DA, Gammons CH, Parker SR. 2011. Diel biogeochemical processes and their effect on the aqueous chemistry of streams: a review. *Chemical Geology* **283**(1-2): 3–17. DOI:10.1016/j.chemgeo.2010.08.017.

O'Callaghan J, Mark D. 1984. The extraction of drainage networks from digital elevation data. *Computer Vision Graphics and Image Processing* **28**(3): 323–344. DOI:10.1016/S0734-189X(84)80011-0.

O'Loughlin EM. 1981. Saturation regions in catchments and their relations to soil and topographic properties. *Journal of Hydrology* **53**: 229–246.

Olaya V. 2004. *A Gentle Introduction to SAGA GIS*, User Manual. The SAGA User Group e.V: Gottingen.

Payn R, Gooseff M, McGlynn B, Bencala K, Wondzell S. 2009. Channel water balance and exchange with subsurface flow along a mountain headwater stream in Montana, United States. *Water Resources Research* **45**: W11427. DOI:10.1029/2008WR007644.

Pilgrim D. 1976. Travel times and nonlinearity of flood runoff from tracer measurements on a small watershed. *Water Resources Research* **12**(3): 487–496. DOI:10.1029/WR012i003p00487.

Rinaldo A, Marani A, Rigon R. 1991. Geomorphological dispersion. *Water Resources Research* **27**(4): 513–525. DOI:10.1029/90WR02501.

Rinaldo A, Vogel GK, Rigon R, Rodriguez-Iturbe I. 1995. Can one gauge the shape of a basin? *Water Resources Research* **31**(4): 119–1127.

Rinaldo A, Beven KJ, Bertuzzo E, Nicotina L, Davies J, Fiori A, Russo D, Botter G. 2011. Catchment travel time distributions and water flow in soils. *Water Resources Research* **47**(7): W07537. DOI:10.1029/2011WR010478.

Robinson JS, Sivapalan M, Snell JD. 1995. On the relative roles of hillslopes processes, channel routing, and network geomorphology in the hydrologic response of natural catchments. *Water Resources Research* **31**(12): 3089–3101.

Rodriguez-Iturbe I, Valdes J. 1979. Geomorphologic structure of hydrologic response. *Water Resources Research* **15**(6): 1409–1420. DOI:10.1029/WR015i006p01409.

Runkel RL. 2015. On the use of rhodamine WT for the characterization of stream hydrodynamics and transient storage. *Water Resources Research* **51**: 6125–6142. DOI:10.1002/2015WR017201.

Saco PM, Kumar P. 2002a. Kinematic dispersion in stream networks 1. Coupling hydraulic and network geometry. *Water Resources Research* **38**(11): 1244. DOI:10.1029/2001WR000695.

Saco PM, Kumar P. 2002b. Kinematic dispersion in stream networks 2. Scale issues and self-similar network organization. *Water Resources Research* **38**(11): 1245. DOI:10.1029/2001WR000694.

Seibert J, McGlynn B. 2007. A new triangular flow direction algorithm for computing upslope areas from gridded digital elevation models. *Water Resources Research* **43**(4): W04501. DOI:10.1029/2006WR005128.

Snell JD, Sivapalan M. 1994. On geomorphological dispersion in natural catchments and the geomorphological unit hydrograph. *Water Resources Research* **30**(7): 2311–2323.

Snell JD, Sivapalan M, Bates B. 2004. Nonlinear kinematic dispersion in channel network response and scale effects: application of the meta-channel concept. *Advances in Water Resources* **27**: 141–154.

Speight JG. 1980. The role of topography in controlling throughflow generation—a discussion. *Earth Surface Processes and Landforms* **5**(2): 187–191. DOI:10.1002/esp.3760050209.

Troutman BM, Karlinger MR. 1984. On the expected width function for topologically random channel network. *Journal of Applied Probability* **21**(4): 836–849.

Troutman BM, Karlinger MR. 1985. Unit hydrograph approximation assuming linear flow through topologically random channel networks. *Water Resources Research* **21**(5): 743–754.

Valdes JB, Fiallo Y, Rodriguez-Iturbe I. 1979. A rainfall–runoff analysis of the geomorphic IUH. *Water Resources Research* **15**(6): 1421–1434.

Wollheim WM, Vörösmarty CJ, Peterson BJ, Seitzinger SP, Hopkinson CS. 2006. Relationship between river size and nutrient removal. *Geophysical Research Letters* **33**(6): . DOI:10.1029/2006GL02584.

Wondzell S, Gooseff M, McGlynn B. 2007. Flow velocity and the hydrologic behavior of streams during baseflow. *Geophysical Research Letters* **34**(24): L24404. DOI:10.1029/WR021i005p00743.

Wondzell S, Gooseff M, McGlynn B. 2010. An analysis of alternative conceptual models relating hyporheic exchange flow to diel fluctuations in discharge during baseflow recession. *Hydrological Processes* **24**(6): 686–694. DOI:10.1002/hyp.7507.

Worrall F, Howden NJK, Moody CS, Burt TP. 2013. Correction of fluvial fluxes of chemical species for diurnal variation. *Journal of Hydrology* **481**: 1–11. DOI:10.1016/j.jhydrol.2012.11.037.

Worrall F, Howden NJK, Burt TP. 2014. A method of estimating in-stream residence time of water in rivers. *Journal of Hydrology* **512**: 274–284.

APPENDIX A.

Table A1. Abbreviations used in text and respective definitions[a]

Abbreviation	Definition
VV	Variable velocity, derived from an empirical relationship between discharge and tracer velocity
CV	Constant velocity, a mean calculated from individual reach velocities in a given watershed
IW	Inflow weighted, incorporating spatially variable water delivery to the stream network
TTF	Travel time function, the approximation of the distribution of travel times from entry to the stream network to the watershed outlet

[a] Some abbreviations are used in combination throughout the text, e.g. IW-TTF.